Tailoring of paramagnetic (structurally ordered) nanometric grains separated by ferromagnetic (structurally disordered) grain boundaries: Isolating grain-boundary magnetic effects

X. Amils, J. Nogués, S. Suriñach, J. S. Muñoz, and M. D. Baró
Departament de Física, Universitat Autònoma de Barcelona, 08193 Bellaterra, Spain

A. Hernando
Inst. Magnetismo Aplicado (RENFE-UCM-CSIC), P.O. Box 155, 28230 Las Rozas, Spain

J. P. Morniroli
Laboratoire de Métallurgique Physique et Génie des Matériaux, UMR CNRS 8517, USTL, 59655 Villeneuve d'Ascq Cedex, France
(Received 29 June 2000; published 4 January 2001)

Partially reordering heavily milled intermetallic alloys results in structurally and chemically ordered nanometric grains separated by structurally and chemically disordered grain boundaries. In systems with disorder induced ferromagnetism this structural microstructure causes a peculiar magnetic microstructure: paramagnetic grains separated by magnetically ordered (ferromagnetic) grain boundaries. This unusual structural-magnetic microstructure allows for the easy separation of the magnetic contribution of the grain boundaries. This contribution is found to be about 15%, suggesting that the grain boundary is a few atomic layers thick, in agreement with high-resolution transmission electron microscopy observations.

DOI: 10.1103/PhysRevB.63.052402 PACS number(s): 75.50.Kj

The magnetic properties of nanometer size particles are of great current interest. From the technological point of view, high-density recording media,[1] giant magnetoresistance,[2] soft magnetic properties,[3] or large coercivities[4] observed in various nanophase materials are the focus of intense research. Moreover, basic phenomena such as quantum tunneling of magnetization[5] or enhanced magnetic moments[6] are also being investigated.

Due to their reduced size, nanometric particles have a considerable percentage of their atoms at the surface or at grain boundaries, with a rearranged atomic configuration (e.g., reduced number of neighbors or disordered arrangements). Hence the surface atoms should strongly affect the overall magnetic properties.[7–9] However, most of the experimentally observed magnetic surface effects at room temperature are difficult to separate from the behavior of the grain. Therefore they are only discernible using very sensitive probes (e.g., Mössbauer spectroscopy[7] or neutron scattering[8]). In most cases, magnetic surface effects are only appreciable at cryogenic temperatures.[9]

Ball milling has achieved widespread application in several research fields as a tool for producing metastable nanocrystalline structures.[10] Particularly, for intermetallic phases, grain refinement and disordering are typical modifications which are brought about during milling.[10]

Ordered Fe-Al alloys are known to become paramagnetic at room temperature for Al concentrations above 30%.[11] However, when these alloys are deformed or disordered they become ferromagnetic. The induction of ferromagnetism has been associated with dislocation nucleation, which is accompanied by the generation of antiphase boundaries over the dislocation glide planes and the rearrangement of Fe atoms from the original $B2$ ordered structure.[12]

In this work, we have studied both ball-milled and bulk compressed Fe-40Al at. % samples. Appropriate thermal treatments in the ball-milled powders allow us to tailor the microstructure to obtain ordered grains (paramagnetic) embedded in disordered grain boundaries (ferromagnetic). Therefore the contribution of the grain boundaries to the magnetic properties can be discerned at room temperature from magnetization measurements.

Two sets of Fe-40Al at. % samples were prepared: (i) atomized powders ball milled for 72 h in a planetary mill under argon using agate vials and zirconia balls and (ii) bulk samples homegenenized at 1473 K for 5 h and then compressed with 50% strain. The samples were characterized by x-ray diffraction (XRD), differential scanning calorimetry (DSC), transmission electron microscopy (TEM), and vibrating sample magnetometry (VSM). The average microstructural parameters were calculated from a full pattern XRD fitting procedure.[13] The local microstructural parameters of the ball milled samples were obtained from selected area electron diffraction (the diffracting area selected by the selected area aperture was in the range $0.2 - 5\ \mu$m) and electron nanodiffraction[14] (the diffracting area was directly defined by a spot size in the range 10–35 nm). Hysteresis loops, up to 10 kOe, were measured at room temperature. The temperature dependence of the dc susceptibility $\chi_{dc} = M/H$ was determined by warming the sample in vacuum at a constant heating rate, $\beta = 1.3$ K/min, up to 750 K. The room-temperature saturation magnetization M_S and the uniaxial anisotropy K_U were estimated from the classical law of approach to saturation.[15]

X-ray results indicate that the as-milled particles are composed of disordered (mainly antisite defects, i.e., point defects) nanometer size grains ($d \sim 13$ nm) embedded in disordered boundaries (mainly linear and planar defects, e.g., networks of dislocations),[15,16] as shown schematically in Fig. 1(a). The grain sizes obtained in the TEM analysis are consistent with the ones obtained from XRD. Two reordering stages are observed upon annealing. First reordering of the grains with minor grain growth takes place ($T_{ann} \leqslant 523$ K,

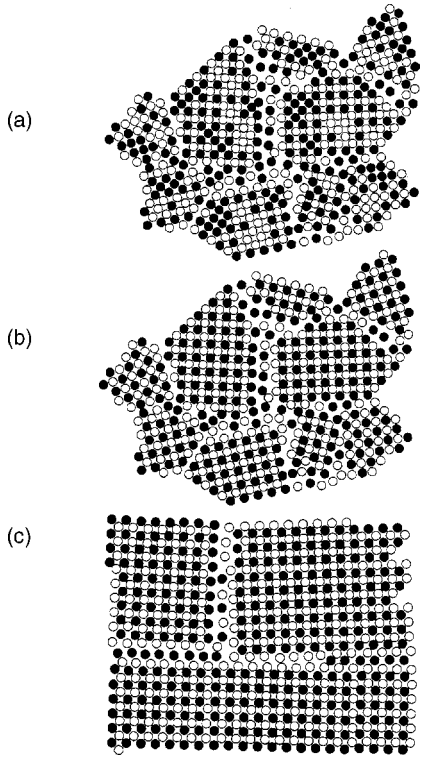

FIG. 1. Schematic representation of the evolution of the atomic arrangement at different stages (a)–(c) of the reordering of ball-milled 72-h FeAl powders.

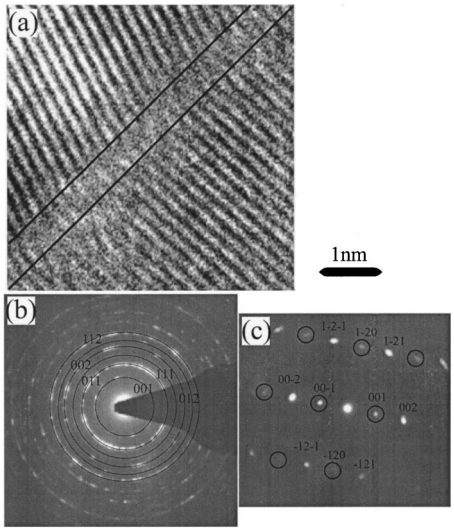

FIG. 2. (a) Transmission electron microscope micrograph of the interface between two FeAl grains (note that the two continuous lines are drawn to highlight the disordered interface area), (b) selected area diffraction ring pattern for a sample ball-milled 72 h and annealed 1 h at $T_{ann}=523$ K. The selected diffracted area size is about 2 μm and the pattern is indexed as an ordered $B2$ structure with $a=0.2909$ nm, and (c) corresponding nanodiffraction spot pattern. The diffracted area is about 35 nm. The pattern is interpreted as an ordered {210} zone axis pattern (ZAP). The superstructure spots are indicated by open circles.

followed by the reordering of the grain boundaries with the concomitant important grain growth at high annealing temperatures[15,16] [shown schematically in Figs. 1(b) and (c)]. Selected area diffraction and nanodiffraction results confirm the results obtained by XRD. For example, we observed that after annealing at $T_{ann}=523$ K the grains transform from a disordered $A2$ structure (as milled) to an ordered $B2$ structure, [see Figs. 2(b) and (c)], with only a small change in average grain size. It is noteworthy that the selected area diffraction pattern is a ring pattern [Fig. 2(b)] due to a random orientation of the nanometric grains within the 5-μm diffracting area. However, the nanodiffraction pattern is a spot pattern [Fig. 2(c)], since the nanometer size of the diffracted area predominantly contains a *unique* or a very reduced number of grains. As can be seen in Fig. 2(b), after annealing, the selected area diffraction ring structure can be indexed as an ordered $B2$ structure [note that superstructure peaks such as (001), (111), or (012) are clearly discernible] with a = 0.2909 nm. Similarly, the nanodiffraction pattern of the annealed samples exhibit usually both fundamental and superstructure peaks [labeled with open circles in Fig. 2(c)] and can be interpreted as a zone axis pattern (ZAP) of an ordered a $B2$ structure, indicating the ordered nature of the grains. Moreover, the high-resolution TEM images also show that the interface between grains remains disordered even after annealing at $T_{ann}=523$ K [Fig. 2(a)]. The DSC results for the 72 h as-milled powders show two transitions around 400 and 700 K (see inset in Fig. 3), which according to XRD results correspond to the reordering and the recrystallization processes, respectively. However, the bulk compressed samples only exhibit a unique transition around 400 K (Fig. 3, inset), with an exothermic release of about 15 J/g, significantly lower than the 50 J/g obtained for the 72 h ball-milled powder.[16] X-ray, electron-diffraction, and DSC analyses indicate that for temperatures above 500 K, point defects are annealed out, i.e., grains reorder in the case of the powders and the whole sample recovers in the case of the bulk compressed samples. This is in agreement with previous TEM observations of forged samples, which do not have enough density of dislocations to form grain boundaries,

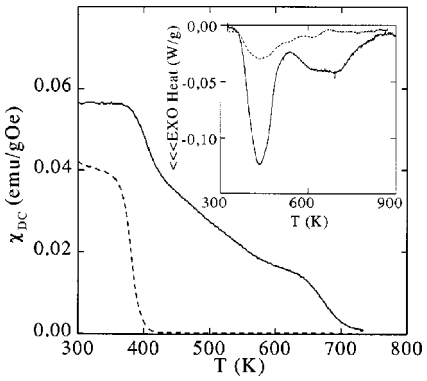

FIG. 3. Temperature dependence of the dc susceptibility χ_{dc}, at $H=0.05$ kOe for the ball-milled 72-h (solid line) and the bulk compressed (dashed curve) samples. Measurements were carried out at $\beta=1.3$ K/min in vacuum. Shown in the inset are the DSC scans for the ball-milled-72 h (solid line) and bulk compressed (dashed line) samples, measured at $\beta=20$ K/min heating rate.

however ball-milled samples contain dislocation networks which act as grain boundaries.[17,18] It is noteworthy that x-ray results indicate that the compressed bulk samples are partially disordered in the as-compressed state. In the case of the ball-milled powders, for temperatures around 500 K, the grain size remains small, although the microstrains (indicative of the existence of dislocations) are high.[15,16] XRD (Ref. 15) and magnetic thermogravimetry Avrami's[19] analyses of the reordering transition indicate that the reordering grows independently inside each nanodomain.[18] Thus, as observed in Fig. 2(a) and as shown schematically in Fig. 1(b), the ball-milled samples annealed at $T_{ann}=523$ K are composed of ordered grains bounded by disordered grain boundaries. Temperatures above 700 K are required to recover the grain boundaries, since significant grain growth and recrystallization takes place at that temperature[15,16] [see Fig. 1(c)]. Thus the microstructure of the ball-milled powder can be tailored to different microstructures depending on the annealing conditions.

The original atomized powders (structurally and chemically ordered) are paramagnetic at room temperature,[20] as expected from their Fe content.[11] The as-milled samples exhibit a rather large saturation magnetization, $M_S=75.4$ emu/g, consistent with their disordered character.[12,20] The temperature dependence of the dc susceptibility χ_{dc} at low fields ($H<H_{Sat}$) for the as-milled samples, shown in Fig. 3, exhibits two steps around $T=400$ and 700 K, respectively. The bulk samples exhibit moderate room-temperature saturation magnetization, $M_S=21.1$ emu/g. Moreover, the temperature dependence of the magnetization at low fields of the bulk compressed samples shows only one step around 400 K. The behavior of the as-milled powders can be understood in terms of the reordering of the different types of defects, as shown in Figs. 1(a)–(c). Around $T=400$ K the point defects are annealed out. Thus the grains reorder [Figs. 1(a) and (b)], hence the grains exhibit a ferromagnetic (structural-chemical disorder) to paramagnetic (structural-chemical order) transition.[15] However, the grain boundaries remain disordered, thus a considerable magnetization remains. Above $T=700$ K, the planar defects are restored, thus there is an important grain growth (i.e., reduction of the volume fraction of the grain boundaries) [Figs. 1(b) and (c)]. Consequently, the contribution of the grain boundaries becomes paramagnetic. In the case of the bulk compressed samples, the whole sample recovers around 400 K. As a result, the sample becomes paramagnetic for temperatures above 400 K. Thus x-ray, DSC, and magnetization results confirm that no grain boundaries are present in bulk compressed samples.

To obtain the room-temperature contribution of the grain boundaries to the overall magnetization, we have, following DSC and magnetization results, annealed the as-milled powders at $T_{ann}=523$ K for 1 h. This procedure allows us to tailor an advantageous structural microstructure where the grains are reordered, however, the grain boundaries continue disordered[15,16] [Figs. 1(b) and 2(a)] Therefore in Fe-40Al at. %, due to the disorder induced ferromagnetism, this leads to an interesting *magnetic* microstructure where the grains should be *paramagnetic* while the grain boundaries should remain magnetically ordered, i.e., *ferromagnetic*. Consequently, due to the paramagnetic character of the grains, the contribution of the grain boundaries to the overall magnetization will be dominating despite their reduced volume. As can be seen in the temperature dependence of the dc-susceptibility after annealing at $T_{ann}=523$ K, given in Fig. 4, only a single transition is observed at about 700 K, i.e., only the grain boundaries contribute to the magnetization. It is noteworthy that above 500 K the curve for the annealed and as-milled samples (see Fig. 4) remain virtually identical, indicating that the grain boundaries have hardly changed after the annealing. From the initial magnetization curve at room temperature (see inset in Fig. 4), after annealing at $T_{ann}=523$ K, the saturation magnetization of the grain boundaries is found to be M_S(boundary)$=11.7$ emu/g. Hence, using M_S from the as-milled grains, the grain boundary contribution to the magnetization is at least 15% of the overall magnetization. However, to estimate the grain-boundary contribution more accurately, other effects of annealing, such as small grain growth, grain-boundary relaxation or lattice parameter changes should be taken into account.[20,21] Unfortunately, it is difficult to estimate the exact volume of the grain boundaries, because due to the different types of defects present in the grains and in the grain boundaries, the magnetization (per unit volume) of the grains could be different from that of the grain boundaries. However, one would expect that (i) the grain boundaries to have a higher density of defects after milling, hence their magnetization per unit volume could be slightly larger than that of the disordered grains and (ii) the atomic density of the grain boundaries could be smaller than that of the grains. Therefore the 15% contribution of the grain boundaries to the magnetization gives us a first approximation of their relative volume. Assuming the same magnetization per unit volume for grains and grain boundaries and spherical grains of about 1100 nm^3 volume (XRD-TEM grain size), we can estimate that the upper bound of the grain-boundary region is only a few atomic layers thick. This is in excellent agreement with the high-resolution TEM image shown in Fig. 2(a), which

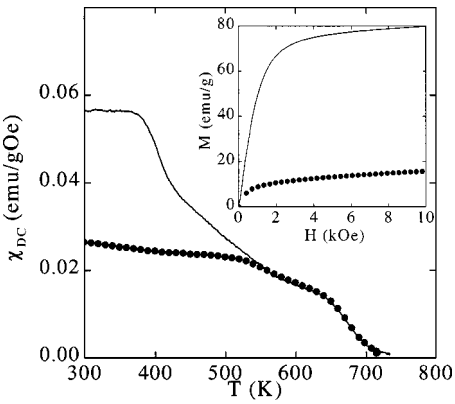

FIG. 4. Temperature dependence of the dc susceptibility χ_{dc} at $H=0.05$ kOe for the ball-milled 72-h (solid line) and the ball-milled 72-h and annealed 1-h at $T_{ann}=523$ K (dotted curve) samples. Measurements were carried out at $\beta=1.3$ K/min in vacuum. The inset shows the initial magnetization curve for the ball-milled 72-h (solid line) and the ball-milled 72-h and annealed 1-h at $T_{ann}=523$ K (dotted curve) samples.

indicates an interface thickness of about 1 nm. These results are also in agreement with theoretical calculations[22] and indirect estimations from Mössbauer measurements[23,24] of intergranular volume fractions.

To confirm these results, we have also studied the coercivity. As the magnetically active length scale becomes smaller than the exchange length, $l_{ex}=(A/K_U)^{1/2}\sim 3$ nm [using $A=10^{-11}$ J/m and $K_U=3.11\times 10^5$ J/m^3 (Ref. 15)], one would expect a hardening of the material. This is indeed the case for our samples, which exhibit an increase of coercivity from the as-milled state, $H_C=50$ Oe, to the annealed state, $H_C=144$ Oe.

In conclusion, we have shown that structural microstructure of ball-milled powders can be customized using different annealing conditions. In particular, ordered nanometric grains embedded in disordered grain boundaries have been obtained. Since Fe-40Al at.% exhibits a disorder induced ferromagnetic transition, by annealing at temperatures between grain reordering and recrystallization of the ball-milled samples we can obtain a different magnetic microstructure, namely, ordered grains (*paramagnetic*) surrounded by disordered grain boundaries (*ferromagnetic*). Therefore, using this special magnetic microstructure, the contribution of the grain boundaries to the total room-temperature magnetization can be obtained. This contribution is about 15%, which implies a grain-boundary thickness of a few atomic layers, in agreement with high-resolution TEM observations.

We wish to thank S. Gialanella and L. Lutterotti for providing the Fe-Al powder samples and for their help in the x-ray-diffraction analysis and Y. Maniette for his help in the TEM imaging. X.A. and J.N. acknowledge the Spanish Government for its financial support. Partial financial support from EU (INTAS-1999-00425), CICYT (MAT98-0730), and DGR (1999SGR00340) is also acknowledged.

[1] S. Onodera, H. Kondo, and T. Kawana, MRS Bull. **21**, 35 (1996).
[2] M.J. Carey *et al.*, Appl. Phys. Lett. **61**, 2935 (1992); J.S. Jiang, J.Q. Xiao, and C.L. Chien, *ibid.* **61**, 2362 (1992).
[3] S. Suriñach *et al.*, Nanostruct. Mater. **6**, 461 (1995); A. Ślawska-Waniewska *et al.*, Phys. Rev. B **50**, 6465 (1994).
[4] J. Löffler *et al.*, Nanostruct. Mater. **9**, 523 (1997); Y.D. Yao *et al.*, *ibid.* **6**, 933 (1995).
[5] W. Wernsdorfer *et al.*, Phys. Rev. Lett. **79**, 4014 (1997).
[6] I.M.L. Billas *et al.*, Phys. Rev. Lett. **71**, 4067 (1993); M. Respaud *et al.*, Phys. Rev. B **57**, 2925 (1998).
[7] L. Del Bianco *et al.*, Phys. Rev. B **56**, 8894 (1997); A. Ślawska-Waniewska and J.M. Grenèche, *ibid.* **56**, R8491 (1997); Y. Sasaki *et al.*, J. Appl. Phys. **81**, 4736 (1997); G. Le Caër and P. Delcroix, Nanostruct. Mater. **7**, 127 (1996).
[8] F. Gazeau *et al.*, Europhys. Lett. **40**, 575 (1997); C. Bellouard, M. Hennion, and Y. Mirebeau, J. Magn. Magn. Mater. **140-144**, 357 (1995); W. Wagner *et al.*, Nanostruct. Mater. **6**, 929 (1995).
[9] R.H. Kodama *et al.*, Phys. Rev. Lett. **77**, 394 (1996); R.H. Kodama, S.A. Makhlouf, and A.E. Berkowitz, *ibid.* **79**, 1393 (1997); B. Martínez *et al.*, *ibid.* **80**, 81 (1998); D. Fiorani *et al.*, J. Magn. Magn. Mater. **157-158**, 159 (1996).
[10] C.C. Koch, *Materials Science Technology*, edited by R.W. Cahn, P. Haasen, and E.J. Kramer (WCH, Weinheim, 1991) p. 193.
[11] A. Taylor and R.M. Jones, J. Appl. Phys. **29**, 522 (1958); A. Arrott and H. Sato, Phys. Rev. **114**, 1420 (1959).
[12] S. Takahashi, X.G. Li, and A. Chiba, J. Phys.: Condens. Matter **8**, 11 243 (1996); Y. Yang, I. Baker, and P. Martin, Philos. Mag. B **79**, 449 (1999).
[13] L. Lutterotti, P. Scardi, and P. Maistrelli, J. Appl. Crystallogr. **25**, 459 (1992).
[14] J.P. Morniroli and J.W. Steeds, Ultramicroscopy **42**, 219 (1992).
[15] X. Amils *et al.*, Mater. Sci. Forum **269-272**, 637 (1998).
[16] S. Gialanella *et al.*, Acta Mater. **46**, 3305 (1998).
[17] M.A. Morris, S. Gunther, and D.G. Morris, Mater. Sci. Forum **269-272**, 631 (1998).
[18] For a recent review on the structural properties of ball-milled intermetallics, see D.G. Morris *et al.*, Int. J. Non-Equil. Process. (to be published).
[19] S. Suriñach *et al.*, Mater. Sci. Forum **235-238**, 415 (1997).
[20] X. Amils *et al.*, IEEE Trans. Magn. **34**, 1129 (1998).
[21] A. Hernando *et al.*, Phys. Rev. B **58**, R11 864 (1998).
[22] G. Palumbo, S.J. Thorpe, and K.T. Aust, Scr. Metall. Mater. **24**, 1347 (1990).
[23] D. Negri, A.R. Yavari, and A. Deriu, Acta Mater. **47**, 4545 (1999).
[24] B. Fultz, H. Kuwano, and H. Ouyang, J. Appl. Phys. **77**, 3458 (1995).